Predicted Ordered Assembly of Ethylene Molecules Induced by Polarized Off-Resonance Laser Pulses

Maxim Artamonov and Tamar Seideman*

Department of Chemistry, Northwestern University, 2145 Sheridan Road, Evanston, Illinois 60208-3113, USA

(Received 2 March 2012; published 17 October 2012)

We illustrate a new phenomenon in the dynamics of molecular ensembles subjected to moderately intense, far-off-resonance laser fields, namely, field-driven formation of perfectly ordered, defect-free assembly. Interestingly, both the arrangement of the constituting molecules within the individual assembly and the long-range order of the assembly with respect to one another are subject to control through choice of the field polarization. Relying on strong induced dipole-induced dipole interactions that are established in dense molecular media, the effect is expected to be general.

DOI: 10.1103/PhysRevLett.109.168302 PACS numbers: 82.53.Kp, 33.20.Xx, 33.80.Wz, 81.16.Dn

Molecular self-assembly is one of the major tools of nanosciences and nanotechnology [1,2] and plays an important role also in natural systems [3,4]. In general, molecular self-assembly relies on a delicate balance between several intermolecular forces, presenting a challenge to numerical modeling [5,6]. Further, the translational and orientational order of the constituting molecules depends sensitively on the chemical properties of constituents and is difficult to control, not uncommonly exhibiting local defects [7,8]. Here we point to a new and fascinating molecular assembly mechanism which, to our knowledge, has not been observed experimentally or numerically before, and which relies on a simple and very general mechanism, namely the induced dipole-induced dipole interaction among molecules subjected to a far-off-resonance laser pulse. The assemblies are defect-free and exhibit long-range orientational and translational order that is subject to control through choice of the laser field polarization. In addition to its fundamental interest, the assembly mechanism may also carry a long-term practical benefit in the design of new materials with preferred electric, magnetic, optical or mechanical properties. This mechanism is related to a family of similar phenomena, where long-range spatial order arises in an ensemble of interacting dipoles. Other examples include formation of clusters in colloidal dispersions of ferromagnetic particles in an external magnetic field [9,10], coarsening of colloidal suspensions of polarizable microparticles in an external electric field [11–13], and self-assembly of cold polar molecules into two-dimensional crystals via repulsive interaction between their dipoles aligned by an external electric field [14].

We envision an ensemble of gas phase molecules subjected to a far-off-resonance, moderately intense (below the off-resonance ionization threshold) laser pulse of long duration with respect to the rotational time scales. Under these conditions, vibrational or electronic excitation does not take place and the laser pulse interacts solely with the polarizability tensor of the molecules, typically giving rise to molecular alignment [15,16]. Related laser-induced phenomena that have been theoretically and experimentally explored in the past and are relevant also to the present contribution include three-dimensional laser alignment of asymmetric top molecules [17–22], torsional control of nonrigid molecules [23–26], and molecular focusing in spatially inhomogeneous laser fields [27–32]. At the root of these phenomena is the interaction of the laser field with the induced dipole of the molecules, essentially the (orientationally and in several cases also spatially inhomogeneous) Stark effect. Under low intensity, low density conditions, the induced dipole-induced dipole interactions among the molecules are negligibly small. As the field-matter interaction strength grows, or the molecular density increases, however, these interactions exceed the thermal energy, expressing themselves in the formation of molecular assembly with unique properties, as illustrated below.

Our results are based on molecular dynamics simulations of an ensemble of rigid, asymmetric top molecules. We describe the interaction between the atoms on any two molecules by the Lennard-Jones (LJ) potential,

$$V_{\mathrm{LJ}} = \sum_{i<j} \sum_{\mu_i,\nu_j} \left[\frac{B_{\mu_i\nu_j}}{r^{12}_{\mu_i\nu_j}} - \frac{A_{\mu_i\nu_j}}{r^{6}_{\mu_i\nu_j}} \right], \tag{1}$$

where i and j run over molecules, μ_i and ν_j run over the atoms on the corresponding molecule, and $r_{\mu_i\nu_j}$ is the distance between atoms μ_i and ν_j. As a simple test case, we consider ethylene molecules, for which the potential parameters are provided in Ref. [33]. As shown below, however, our conclusions are entirely general. The applied laser field, $\boldsymbol{\epsilon}(t)$, induces dipoles on the molecules, $\mathbf{d} = \boldsymbol{\alpha}\boldsymbol{\epsilon}(t)$, with $\boldsymbol{\alpha}$ denoting the molecular polarizability tensor in the space-fixed (SF) frame. The induced dipoles interact with the laser field and with each other, giving rise to the induced potential, V_{ind},

$$V_{\mathrm{ind}} = -\frac{1}{2}\sum_i \Big[\Re\{\mathbf{d}_i \cdot \boldsymbol{\epsilon}(t)^*\} + \frac{1}{4\pi\varepsilon_0 r_{ij}^3} \times \sum_{j\neq i} \Re\{3(\mathbf{d}_i \cdot \mathbf{n}_{ij})(\mathbf{n}_{ij} \cdot \mathbf{d}_j^*) - \mathbf{d}_i \cdot \mathbf{d}_j^*\} \Big], \quad (2)$$

where ε_0 is the permittivity of free space, and $\Re\{\}$ and $*$ denote the real part and the complex conjugate, respectively. In Eq. (2), $\mathbf{r}_{ij}$ is the vector between the centers of mass (c.m.) of molecules i and j, $\mathbf{r}_{ij} = \mathbf{r}_i - \mathbf{r}_j$, $r_{ij} = |\mathbf{r}_{ij}|$, and $\mathbf{n}_{ij}$ is a unit vector along $\mathbf{r}_{ij}$. Our theory and numerical method are discussed in detail in the Supplemental Material [34], where we also provide the computational parameters.

Essential to the formation of orientationally ordered assembly are the phenomena of laser-induced alignment and three-dimensional alignment. It is thus germane to open the discussion of our results with a brief description of the alignment dynamics in a molecular ensemble within the classical approximation. We use the conventional alignment measures, $\langle\cos^2\theta\rangle(t)$, $\langle\cos^2\phi\rangle(t)$, and $\langle\cos^2\chi\rangle(t)$ to quantify the degree of (1D or 3D) alignment and its time evolution, where θ, ϕ, and χ are the Euler angles of rotation between the SF and body-fixed (BF) frames, and follow the conventions of Zare [35]. The BF Z axis is defined by the CC bond, with the Y axis lying in the molecular plane. The SF z axis is defined, as conventional, by the field polarization vector in the case of linear polarization and by the field k vector in the cases of circular and elliptical polarization.

Figure 1 shows the results of a simulation with 128 molecules in a cubic box with a side of 100 Å (0.213 mol L^{-1} density) and the temperature maintained at 200 K. (We note that in the perfect gas limit, the corresponding pressure is 0.353 MPa. The density and pressure are thus significantly below the 0.303 mol L^{-1} density and 0.456 MPa pressure [36] of saturated ethylene vapor at 200 K.) The temperature is maintained using the Berendsen thermostat [37] with a relaxation time constant of 2.4 ps [38]. Before the pulse turn-on, the averages of the squared cosines of the Euler angles are at their isotropic rotational distribution values, $\langle\cos^2\theta\rangle = 1/3$ and $\langle\cos^2\phi\rangle = \langle\cos^2\chi\rangle = 1/2$. Upon the pulse turn-on, in the linear polarization case, the most polarizable molecular axis, Z, aligns with the field polarization direction, producing sharp alignment in θ with $\langle\cos^2\theta\rangle \sim 0.9$. With the other two polarizations, the Z axis aligns with the field polarization plane, xy, leading to sharp antialignment in θ with $\langle\cos^2\theta\rangle < 0.1$. Both linearly and circularly polarized fields possess cylindrical symmetry about the SF z axis and thus cannot produce alignment in ϕ. Conversely, with an elliptically polarized field, the most polarizable axis aligns with the major axis of the polarization ellipse whereas the second most polarizable axis aligns with the minor axis of the ellipse, yielding substantial alignment in ϕ with $\langle\cos^2\phi\rangle \sim 0.8$. The relatively weak alignment in χ compared to the much sharper alignment in ϕ in the case of the elliptically polarized field is the result of the small polarizability anisotropy in the molecular XY plane of ethylene. This small anisotropy affords little coupling with the aligning field and, consequently, little hindrance to rotation about the molecular Z axis. Figure 1 compares well with the results of quantum-mechanical calculations [20] for a general asymmetric top molecule. (The purely classical approach, applied in the present work in order to treat an ensemble of interacting molecules, cannot account for the wave packet coherent dephasing and revivals that ensue in nonadiabatic alignment induced by a short pulse. In the case of adiabatic alignment considered here, however, the classical framework is expected to provide a reasonable approximation.)

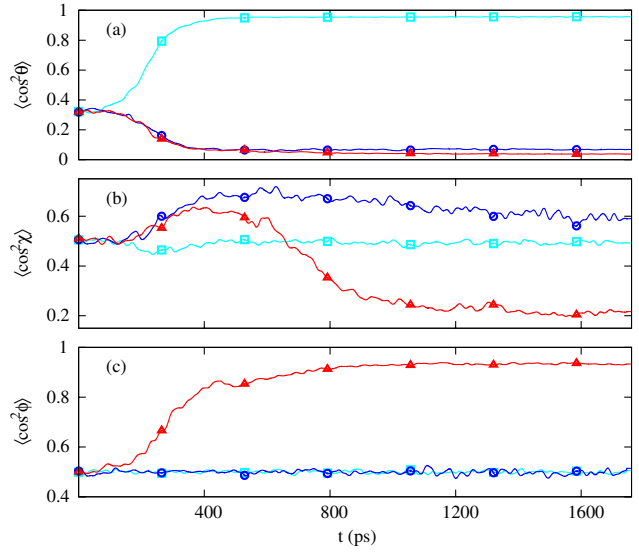

FIG. 1 (color online). Alignment and 3D alignment produced by linearly (cyan, squares), circularly (blue, circles), and elliptically (red, triangles) polarized fields. The field intensity is maintained at the peak value of 110 TW cm^{-2} after the 440 ps turn-on time.

On the time scale of the pulse turn-on, $t \leq 400$ ps, the alignment dynamics is essentially unaffected by the induced dipole–induced dipole interactions, and the interaction between induced dipoles contributes little to the mean values of the induced potential energy, as confirmed by a repeat calculation where these interactions are omitted. As time progresses, however, the attraction between induced dipoles in the head-to-tail configuration overcomes the translational energy, drawing the molecules into chainlike clusters. As the molecules move closer to each other, the dipole-dipole interactions grow stronger, increasing the attractive forces on the c.m., which, in turn, act to further focus the molecules in space. The assembly of molecules produced by these interactions is manifest in lowering of the LJ energy, that is, the ensemble average of V_{LJ}, see Fig. 2(a), which arises from the fact that a large proportion of the molecules settle in the attractive region of the LJ potential. The assembly-driven stabilization, which expresses itself in lowering of the LJ energy, is the most

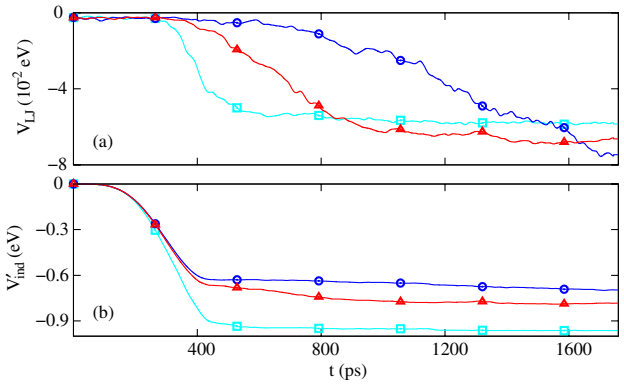

FIG. 2 (color online). Time evolution of the mean Lennard-Jones and the interaction energy between induced dipoles in the course of laser alignment induced by linearly (cyan, squares), circularly (blue, circles), and elliptically (red, triangles) polarized fields. The time profile of the field intensity is as in Fig. 1.

dramatic in the case of linearly polarized field. The polarization dependence and its implications are explained below. The ensemble averaged V_{ind} shows the effects of clustering, as well. The dominant contribution to V_{ind} is from the induced dipole-external field interaction, see Eq. (2); however, the induced dipole-induced dipole interaction strength increases as the molecules come closer together. This is evidenced in the lowering of the ensemble averaged interaction energy between induced dipoles, V'_{ind} in Fig. 2(b), past the 440 ps pulse turn-on time. The assembly formation has a major effect on the molecular alignment characteristics, as the alignment of isolated molecules is transformed into a collective phenomenon that translates, as shown below, into long-range translational and orientational order. These dynamics are illustrated in Fig. 1, where the system is allowed to evolve past the time of the pulse envelope peak with the field intensity maintained at its peak value.

Figure 2 illustrates that field-induced assembly occurs for all three field polarizations but at different rates, with linear and circular polarizations producing, respectively, the most rapid and the slowest decrease in V_{LJ}. The degree of stabilization, which serves as an indicator of the average number of close neighbors a molecule has in an assembly, depends on the polarization in the reverse order. Assembly becomes more compact in going from linear to elliptical to circular polarization. Figures 2(a) and 2(b) show that assembly enhances the interaction between induced dipoles for all three polarizations, with the linear polarization, however, having the greatest effect. The difference between the three polarization cases may have been anticipated, as the polarizability tensor of ethylene exhibits one relatively large and two similar and much smaller BF components. Whereas the circularly polarized field aligns the molecule to the polarization plane and the elliptically polarized one establishes 3D alignment, the linearly polarized field is the most effective in aligning the CC bonds along a unique direction, inducing dipoles in that direction and hence establishing relative order of the molecules with respect to one another. (A more general effect contributing to the observed polarization dependence is that the field-matter interaction is stronger in the linear polarization case, as the field oscillates along a single, rather than two, spatial axis.)

Once the molecules begin to assemble into spatially organized formations, the averaged values of the squared cosines of the Euler angles begin to show the effects of long-range collective ordering. This expresses itself in overall improvement of the alignment. Whereas the sharpening of the θ alignment is moderate, [Fig. 1(a)], a major change in the ϕ alignment is observed in the case of elliptical polarization, [Fig. 1(c)]. The χ alignment is only slightly modified by the assembly formation with the circularly polarized field, whereas in the case of elliptical polarization the sense of alignment in χ is reversed from a modest alignment to sharp antialignment [Fig. 1(b)]. With the most polarizable molecular axis aligned parallel to the major axis of the field polarization ellipse, the most energetically favorable configuration is with the largest component of the induced dipoles arranged head-to-tail, resulting in the molecules lining up like links in a chain. This arrangement forces the second largest component of the induced dipoles, resultant from the alignment of the second largest molecular polarizability component to the direction of the minor axis of the polarization ellipse, into a repulsive configuration. To minimize the repulsion between these induced dipole components on neighboring molecules, the second most polarizable molecular axis is ejected from the field polarization plane leading to the observed antialignment in χ.

Increasing the gas density increases the frequency of the intermolecular encounters and thus the rate of assembly formation. Comparison of the results of simulations performed on ensembles with 128 and 384 molecules in a 100 Å cubic box illustrates that the signatures of assembly formation, namely, inflection of the $\langle \cos^2 \chi \rangle$ curve and lowering of the LJ energy, occur earlier and proceed faster the denser the ensemble. By the time the field envelope peaks (440 ps), all of the properties of the ordered assembly have reached their final values. While accelerating the formation of assembly, tripling the molecular density does not alter the alignment dynamics in any significant way, the squared cosines of Euler angles converging to similar values to those illustrated in Fig. 1.

The field polarization controls also the arrangement of molecules within the clusters, suggesting potential design opportunities. Figures 3 and 4 show snapshots of the 384-molecule ensemble at the end of the simulation for the elliptically and linearly polarized fields, respectively. As with the results of Figs. 1 and 2, the field intensity was maintained at its peak value after the pulse envelope peak to allow the translational degrees of freedom to equilibrate. In the case of an elliptically polarized field, the molecules assemble into *sheets* one molecule thick with their c.m. essentially confined to the same xy plane, the CC bonds

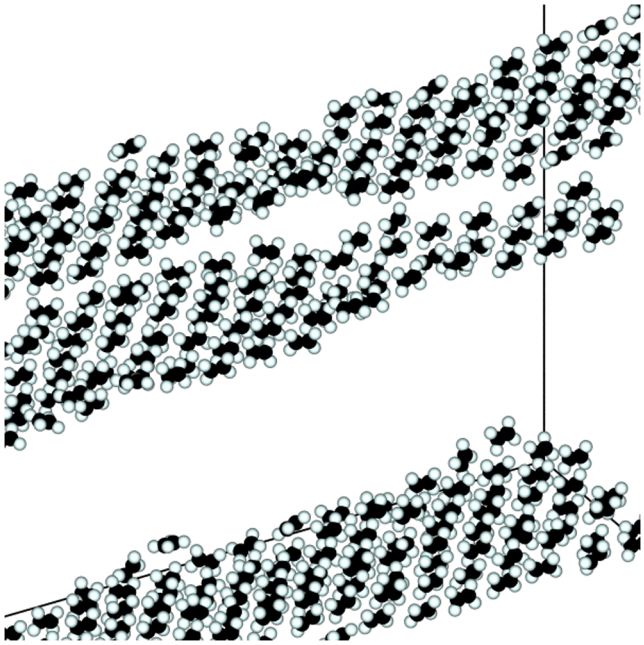

FIG. 3 (color online). A snapshot of a simulation box with 384 molecules at the end of the simulation. The field is elliptically polarized with a peak intensity of 110 TW cm^{-2} maintained for the rest of the simulation.

aligned parallel to the SF x axis, and the CH bonds parallel to the SF zx plane. The neighboring rows in each sheet are arranged with the molecular planes facing each other and their c.m. separated by about 3.9 Å (determined from the pair distribution function, not shown) and staggered. In the same row, that is, along the SF x axis, the molecules are about 5 Å apart. The molecular formations induced by an

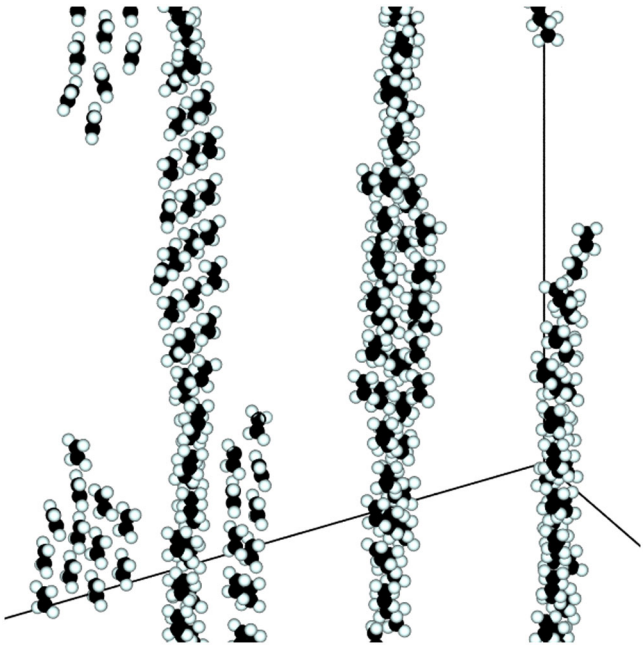

FIG. 4 (color online). As in Fig. 1, but for a linearly polarized field.

elliptically polarized field maintain their structure over time. The "ribbons" formed in the case of a linearly polarized field (Fig. 4) are similar except that the strings of molecules are aligned parallel to the SF z axis, and their lateral extent is smaller, with only a few strings forming individual clusters. In a string, the c.m. are spaced about 5 Å apart, and the vector connecting the c.m. of individual molecules in neighboring strings is ca. 3.8 Å long. In addition, the ribbons can twist about the SF z axis. In the case of a circularly polarized field, the molecular aggregates exhibit size asymmetry with greater expanse in the xy plane than in the z direction but, as expected, appear orderless otherwise.

Detailed examination of the laser intensity and system temperature effects on both the (1D or 3D) alignment and the molecular assembly phenomenon illustrates, as expected, that both parameters play important and competing roles. Whereas the intensity and temperature effects on the alignment are straightforward in the adiabatic domain of relevance, and differ relatively little in the ensemble case from their well-studied [15,16] analogs in isolated molecules, the effect of these parameters on the assembly dynamics is more subtle. At a very qualitative level, one expects laser-induced assembly whenever the density, the laser intensity, and the molecular polarizability tensor are sufficiently large for the induced dipole-induced dipole interaction to be comparable to, or larger than, the thermal energy. Thus, the more polarizable the molecular constituents, the lower the intensity threshold for assembly formation for a given temperature and density. The last point is of practical significance because the maximum practical intensity of the laser field is limited by the onset of undesired processes, such as tunneling ionization. A molecule with large polarization anisotropy, therefore, would make a better potential candidate for experimental realization. While energetic considerations provide a rough guideline, detailed analysis of the effects of temperature, intensity, pulse duration, and field polarization reveals that the assembly phenomenon relies on a delicate interplay between kinetic and dynamic components. We remark that both the spatial and the orientational order are available while the molecules are subject to the laser field. One approach to transforming these effects into permanent order is to adsorb the assembly onto an appropriate substrate [39]. Another is to photoinduce a chemical reaction that will affect polymerization [40].

Summarizing, we point out a fascinating phenomenon in the dynamics of molecular ensembles subject to moderately intense laser pulses, which may have important implications and applications in several subdisciplines of physics, chemistry, and material sciences, namely, purely laser-induced molecular assembly. Specifically, at sufficiently large values of the field-matter interaction, the induced dipole-induced dipole interactions among molecules give rise to field-induced clustering of the molecules into molecular assembly with both long-range translational and long-range orientational order. The inner structures of

the assembly, as well as their shape and relative orientation, can be controlled by choice of the field polarization, suggesting new opportunities for material design. In turn, the assembly process enhances the molecular alignment as compared to the isolated molecule case, unraveling a collective alignment phenomenon. At given values of the field-matter interaction, assembly is encouraged by high density and discouraged by high temperatures. The observation of purely laser-induced molecular assembly exhibiting controllable translational and orientational order may lead to interesting applications in several subdisciplines of physics, chemistry, materials science, and possibly engineering, since translational and orientational order play a major role in determining the electric, magnetic, optical, and mechanical properties of matter.

We are grateful to the Department of Energy (Grant No. DE-FG02-04ER15612) for support.

*t-seideman@northwestern.edu

[1] K. Ariga, X. Hu, S. Mandal, and J. P. Hill, Nanoscale **2**, 198 (2010).
[2] S. Mann, Nature Mater. **8**, 781 (2009).
[3] F. Chiti and C. M. Dobson, Annu. Rev. Biochem. **75**, 333 (2006).
[4] C. Tamerler and M. Sarikaya, Phil. Trans. R. Soc. A **367**, 1705 (2009).
[5] W. F. van Gunsteren, D. Bakowies, R. Baron, I. Chandrasekhar, M. Christen, X. Daura, P. Gee, D. P. Geerke, A. Glttli, P. H. Hnenberger *et al.*, Angew. Chem., Int. Ed. **45**, 4064 (2006).
[6] M. McCullagh, T. Prytkova, S. Tonzani, N. D. Winter, and G. C. Schatz, J. Phys. Chem. B **112**, 10 388 (2008).
[7] R. A. Farrell, T. G. Fitzgerald, D. Borah, J. D. Holmes, and M. A. Morris, Int. J. Mol. Sci. **10**, 3671 (2009).
[8] A. A. Volkert, V. Subramaniam, M. R. Ivanov, A. M. Goodman, and A. J. Haes, ACS Nano **5**, 4570 (2011).
[9] M. Aoshima and A. Satoh, Model. Simul. Mater. Sci. Eng. **16**, 015004 (2008).
[10] D. Heinrich, A. R. Goni, and C. Thomsen, J. Chem. Phys. **126**, 124701 (2007).
[11] A. Yethiraj and A. van Blaaderen, Nature (London) **421**, 513 (2003).
[12] J. E. Martin, R. A. Anderson, and C. P. Tigges, J. Chem. Phys. **108**, 3765 (1998).
[13] J. E. Martin, R. A. Anderson, and C. P. Tigges, J. Chem. Phys. **108**, 7887 (1998).
[14] H. P. Büchler, E. Demler, M. Lukin, A. Micheli, N. Prokof'ev, G. Pupillo, and P. Zoller, Phys. Rev. Lett. **98**, 060404 (2007).
[15] T. Seideman and E. Hamilton, Adv. At. Mol. Opt. Phys. **52**, 289 (2005).
[16] H. Stapelfeldt and T. Seideman, Rev. Mod. Phys. **75**, 543 (2003).
[17] J. J. Larsen, K. Hald, N. Bjerre, H. Stapelfeldt, and T. Seideman, Phys. Rev. Lett. **85**, 2470 (2000).
[18] K. F. Lee, D. M. Villeneuve, P. B. Corkum, A. Stolow, and J. G. Underwood, Phys. Rev. Lett. **97**, 173001 (2006).
[19] E. Hertz, D. Daems, S. Guerin, H. R. Jauslin, B. Lavorel, and O. Faucher, Phys. Rev. A **76**, 043423 (2007).
[20] M. Artamonov and T. Seideman, J. Chem. Phys. **128**, 154313 (2008).
[21] A. Rouzée, S. Guérin, O. Faucher, and B. Lavorel, Phys. Rev. A **77**, 043412 (2008).
[22] S. S. Viftrup, V. Kumarappan, L. Holmegaard, C. Z. Bisgaard, H. Stapelfeldt, M. Artamonov, E. Hamilton, and T. Seideman, Phys. Rev. A **79**, 023404 (2009).
[23] S. Ramakrishna and T. Seideman, Phys. Rev. Lett. **99**, 103001 (2007).
[24] C. B. Madsen, L. B. Madsen, S. S. Viftrup, M. P. Johansson, T. B. Poulsen, L. Holmegaard, V. Kumarappan, K. A. Jørgensen, and H. Stapelfeldt, Phys. Rev. Lett. **102**, 073007 (2009).
[25] C. B. Madsen, L. B. Madsen, S. S. Viftrup, M. P. Johansson, T. B. Poulsen, L. Holmegaard, V. Kumarappan, K. A. Jorgensen, and H. Stapelfeldt, J. Chem. Phys. **130**, 234310 (2009).
[26] S. M. Parker, M. A. Ratner, and T. Seideman, J. Chem. Phys. **135**, 224301 (2011).
[27] T. Seideman, J. Chem. Phys. **107**, 10 420 (1997).
[28] T. Seideman, J. Chem. Phys. **106**, 2881 (1997).
[29] E. Gershnabel and I. S. Averbukh, Phys. Rev. A **82**, 033401 (2010).
[30] R. Gordon, L. Zhu, W. Schroeder, and T. Seideman, J. Appl. Phys. **94**, 669 (2003).
[31] H. Sakai, A. Tarasevitch, J. Danilov, H. Stapelfeldt, R. W. Yip, C. Ellert, E. Constant, and P. B. Corkum, Phys. Rev. A **57**, 2794 (1998).
[32] H. Chung, B. Zhao, S. Lee, S. Hwang, K. Cho, S. Shim, S. Lim, W. Kang, and D. Chung, J. Chem. Phys. **114**, 8293 (2001).
[33] G. Taddei and E. Giglio, J. Chem. Phys. **53**, 2768 (1970).
[34] See Supplemental Material at http://link.aps.org/supplemental/10.1103/PhysRevLett.109.168302 for theory and numerical implementation.
[35] R. N. Zare, *Angular Momentum* (Wiley, New York, 1988).
[36] M. Jahangiri, R. T. Jacobsen, R. B. Stewart, and R. D. McCarty, J. Phys. Chem. Ref. Data **15**, 593 (1986).
[37] H. J. C. Berendsen, J. P. M. Postma, W. F. van Gunsteren, A. DiNola, and J. R. Haak, J. Chem. Phys. **81**, 3684 (1984).
[38] J. Genzer and J. Kolafa, J. Mol. Liq. **109**, 63 (2004). We performed a control simulation with the relaxation time constant increased to 24 ps. While the thermostat efficiency decreased, the alignment and clustering dynamics showed no qualitative differences.
[39] I. Nevo, S. Kapishnikov, A. Birman, M. Dong, S. R. Cohen, K. Kjaer, F. Besenbacher, H. Stapelfeldt, T. Seideman, and L. Leiserowitz, J. Chem. Phys. **130**, 144704 (2009).
[40] H. Menzel, S. Horstmann, M. Mowery, M. Cai, and C. Evans, Polymer **41**, 8113 (2000).